



Artificial Neural Network and Near Infrared Light in Water pH and Total Ammonia Nitrogen Prediction

Nur Aisyah Syafinaz Suarin¹, Jia Sheng Lee¹, Kim Seng Chia^{1*}, Siti Fatimah Zaharah Mohammad Fuzi², Hasan Ali Gamal Al-Kaf³,

¹Faculty of Electrical and Electronic Engineering, Universiti Tun Hussein Onn Malaysia, 86400 Parit Raja, Johor, MALAYSIA

²Oasis Integrated Group, I2E, Universiti Tun Hussein Onn, 86400 Parit Raja, Johor, MALAYSIA

³Universiti Teknologi PETRONAS, Seri Iskandar, MALAYSIA

*Corresponding Author

DOI: <https://doi.org/10.30880/ijie.2022.14.04.017>

Received 12 May 2021; Accepted 11 August 2021; Available online 20 June 2022

Abstract: Water quality plays an important role in aquaculture. The operation of a freshwater aquaculture fish farming is highly dependent on the ability to understand, monitor, and control the physical and chemical constituents of the water. pH and total ammonia nitrogen (TAN) levels are two critical water quality parameters that affect fish growth rate and health. However, pH and TAN levels are affected by uncontrollable factors e.g. weather, temperature, and biological processes occurring in the water. Therefore, it is important to monitor changes in pH and TAN levels frequently to maintain optimal conditions for freshwater habitats. Near infrared spectroscopy (NIR) has been extensively investigated as an alternative measurement approach for rapid quality control without sample preparation. Therefore, this research aims to evaluate the feasibility of machine learning combined with NIR light in predicting the water pH and TAN values of a fish farming system. The proposed system contains three main components i.e. a multi-wavelength light emitting diode (LED), a light sensing element, and a machine learning model i.e. artificial neural network (ANN). First, the transmitted NIR light with different wavelengths of water samples was measured using the proposed system. Then, the actual pH and TAN values of the water samples were quantified using conventional methods. Next, ANN was used to correlate the measured NIR transmittance with the pH and TAN values. The results show that ANN with four hidden neurons achieved the best prediction performance with a mean square error (MSE) of 0.1466 and 0.3136 and a correlation coefficient (R) of 0.8398 and 0.9560 for the pH and TAN predictions, respectively. These results show that ANN coupled with NIR light can be promisingly developed for in situ water quality prediction without sample preparation.

Keywords: Artificial Neural Network, Near Infrared Light, Total Ammonia Nitrogen, pH, Multiple Wavelengths

1. Introduction

Aquaculture is the farming of aquatic organisms to meet up the demands of the world's growing population in a sustainable way. Fish, crustaceans and molluscs are among the aquatic animals involved. They are a source of food, especially protein, for humans. Global aquaculture production has increased rapidly and has surpassed beef production

[1]. Due to the growth of human population, a food crisis has emerged in the world [2]. One of the promising solutions to the food crisis is aquaculture, which can produce a sustainable food supply with an environmentally friendly solution [3]. In the field of aquaculture, fish farming has accounted for more than a quarter of the total fish consumption of people and represents a high-value market in the world [3]. In the earlier years of the fish farming industry, fish were farmed in the seas and rivers, which may have an impact on the environment in the long run. However, nowadays, fish farming can be done in lakes, ponds, and tanks. In the enclosure of fish farming, maintaining an optimal range of physical and chemical conditions of water is extremely important. Different species of fish require different specific water quality ranges for growth, breeding, and survival [4]. Since fish is a living organism, the composition of water changes over time according to the life process and cycles [5]. The composition of water is constantly changing, so water quality monitoring is an important activity that needs to be done frequently. Therefore, water quality monitoring should be a routine activity to ensure that the basic needs of fish for survival are adequately met. Imbalance and large discrepancy between the measurement and the optimal range of water quality may affect fish behaviour and growth, which also increases the risk of fish mortality if the conditions persist for a long time [6], [7].

pH and ammonia are among the two of the most important water quality attributes in fish farming [8]–[10]. The pH is a scale measure (i.e. from 1 to 14) that distinguishes the acidity and basicity of a system. The pH is determined by the activation of hydrogen ion concentration [11]. Different types of aquatic organisms prefer different pH ranges to live, and an aquatic organism may not be able to survive if the pH changes [12]. For instance, the growth rate of mussels (an aquatic organism) would decrease by 50% when the pH falls below 7.5; while most farmed fish die in water with a pH that is below 4.5 or above 10.0 [4], [13]. In fact, a critical imbalance of pH (i.e. pH is lower than 6.0) will cause the loss of beneficial bacteria that are useful for supporting the Nitrogen cycle in water. This could endanger the aquaculture habitat and aquatic organisms. Consequently, this condition will increase toxic ammonia levels in the water [10]. Moreover, according to a study conducted by Ahmad Anas [14] in 2019, the rate of corrosion is highly independent of the pH in the water. This indicates that pH monitoring is crucial to ensure that there is no corrosion in the water that affects the aquaculture equipment, e.g. water pumps, metal pipes, and tanks. In other words, a system that can monitor and maintain an appropriate pH range is of utmost importance to aquaculture.

Next, nitrogen compounds, which in aquaculture occur mainly as ammonia, in aquaculture are contributed by the waste of the fish and the decomposition of the leftover feeds [13]. This nutrient is eventually released into the environment as waste and could have a detrimental effect on ecosystems, including an increase in total suspended solids as well as water turbidity. If ammonia is not treated before it is released into the environment, it is highly toxic and ubiquitous in water [15]. Ammonia can exist in free form (i.e. NH_3) under acidic conditions and in the unionized form, ammonium (NH_4^+). Free ammonia (NH_3) is more toxic compared to ammonium (NH_4^+). The combination of NH_3 and NH_4^+ is called total ammonia nitrogen (TAN). When the pH is in the neutral range, i.e. between 7.0 and 7.5, the value of TAN is mainly contributed by ammonium, which is relatively less toxic. Nevertheless, the value of TAN may increase the value of pH and make more unionized ammonia formed. This can lead to a worsening situation as it will also increase the toxicity of the water. This is because most beneficial bacteria do not survive when the pH is not at the optimal level, and consequently, the biofiltration process of ammonia is slowed down or even stopped [4].

Fish has varying tolerances to ammonia nitrogen; particularly, the concentration of ammonia equal to or more than 0.6 ppm begins to kill most fish species [16]. Since both NH_3 and NH_4^+ are colourless, it is extremely difficult to be seen by naked eyes [13] and cannot be detected individually; there is a need to develop a measurement system that monitors both TAN and pH levels so that the pH-ammonia toxicity relationship can be established to monitor water quality. Recently, research has been proposed to measure ammonia in water using mid and far infrared spectrum [17]. Although the method requires to extract vaporized gas from water by using a complex device, the research succeeds in showing a new approach to measure TAN in water.

Near infrared spectroscopy (NIRS) is a rapid and non-invasive method for assessing physical and chemical compositions. It can reduce the cost of routine analysis by establishing the relationship between near infrared (NIR) energy (i.e. from 750 to 2500 nm) and the components of interest, e.g. ammonia, phosphate, and iron of water [18], [19]. Previous studies have been conducted to study NIRS with the chemical composition of aquaculture solid waste [20], the freshness of freshwater fish [21], surface water qualities [22], process water quality [23], pH and concentration of ammonia [24]. However, the cost of using NIRS is high because it requires a NIR spectrometer to acquire NIR spectra; a halogen lamp to provide a stable light source; a processor, e.g. a computer to process and analyze the acquired NIR spectral data; and a software algorithm to establish the relationship and to develop a predictive model with good performance.

Nowadays, the ability of machine learning to learn complex data, e.g. from spectroscopy, has been improving and is promising for future applications [25], [26]. The information embedded in NIR signals is highly correlated and overlaps with each other. Therefore, robust machine learning is required to establish a good predictive model. There are plenty of machine learning algorithms that can be applied, e.g. Support Vector Machine (SVM) and Partial Least Square (PLS) algorithm [27], [28]. When a machine learning algorithm is applied to analyze NIR signals for chemical prediction, this process is known as chemometrics. There are many chemometrics analyses that have demonstrated their ability to develop a reliable predictive model for the NIRS dataset. Among them, Partial Least Squares (PLS), Principal Component Analysis (PCA), and Artificial Neural Network (ANN) are the common analytical techniques that used in the previous

studies to develop a calibration model for NIRS for fruits, vegetables, and soils [27], [29], [30]. The predictive model for Nitrogen in soil and contamination of nitrate and sulphate were established by using ANN [30], [31]. The ability of ANN to develop a good predictive model was measured by the relative mean square error (RMSE) value. Both studies showed good results with low RMSE value, i.e. 0.0031 for the predictive model of Nitrogen in soil and 0.0132 for the predictive model of nitrate and sulphate contamination. In short, an artificial neural network (ANN) is one of the most well-known nonlinear calibration techniques that can model almost all kinds of complex nonlinear data on the components of interest. ANN has been applied in numerous prediction and classification studies [32]–[34]. However, both overfitting and underfitting must be avoided to fully reveal the capabilities of ANN using appropriate validation approaches.

Recently, the development of advanced light-emitting diode technology (LED), which can emit NIR light with multiple specific wavelengths from a single LED, seems to be promising for detecting NIR energy without an expensive spectrometer and NIR light source [35]. Thus, this research aims to evaluate the feasibility of machine learning coupled with a proposed NIR light acquisition system in predicting the water pH and TAN values of a fish farming system. The objectives of this research are to study the acquired NIR light from water samples using the NIR light acquisition system and to establish the relationship between the acquired NIR light and the water pH and TAN values using ANN.

2. Materials and methods

2.1 System design

Fig. 1 shows the developed prototype of NIR transmission data acquisition for pH and TAN prediction. The prototype consists of two main parts, i.e. (a) the control circuit and (b) the measurement sections. The control circuit section contains a microcontroller, variable resistors, fixed resistors, and step-down voltage regulators, which regulate the $12V_{DC}$ supply to $5V_{DC}$ and to $3.3V_{DC}$ for the multiple wavelengths LED and the microcontroller, respectively. Variable resistors were used to tune the intensity of the LED to avoid signal saturation. The measurement section that was designed to collect the transmitted NIR light contains a light sensing element (i.e. a photodiode), the multiple wavelengths LED (i.e. 670, 770, 810, and 950 nm), and a square cuvette (with a dimension of 10 x 10 x 45 mm). The developed prototype was interfaced using a laptop computer to store, process, analyze, and model the acquired data.

2.2 Spectral Acquisition

First, water samples were collected from an aquarium tank and stored in the square cuvette of the proposed system. The cuvette was positioned between the LED and the photodiode for data acquisition in transmission mode. A black box was used to isolate the sensing components and minimize the occurrence of unwanted signals from the environment. When the proposed system was activated, the LED emitted each wavelength once towards the sample, starting at 670 nm, followed by 770, 810, and 950 nm. On the opposite side, the photodiode measured the intensity of the transmitted NIR light with respect to the specific wavelength. Consequently, the amount of energy absorbed by the samples with respect to the different wavelengths was determined. According to the third overtone region in the NIR band assignment, the NIR light at 770, 810, and 950 nm consists of ROH and CH, RNH_2 and $RNHR$, and ArOH information, respectively. This data acquisition process was repeated five times for each wavelength. The measured transmitted light intensity was transferred from the microcontroller to a laptop computer via a USB cable for Universal Asynchronous Receiver-Transmitter (UART) communication. In each data acquisition, pure water was used to calibrate the sensing system. The spectral from the pure water was collected using the same procedure for water samples. Besides, the same pure water was used to calibrate the sensing system each day. This signal calibration process is important to ensure the acquired signals were referring to the same baseline. This data acquisition was conducted 12 times per day in different time frames over 22 days. Thus, a total of 264 data were recorded. After that, all the collected data were averaged using MATLAB software and would be used as the input of ANN.

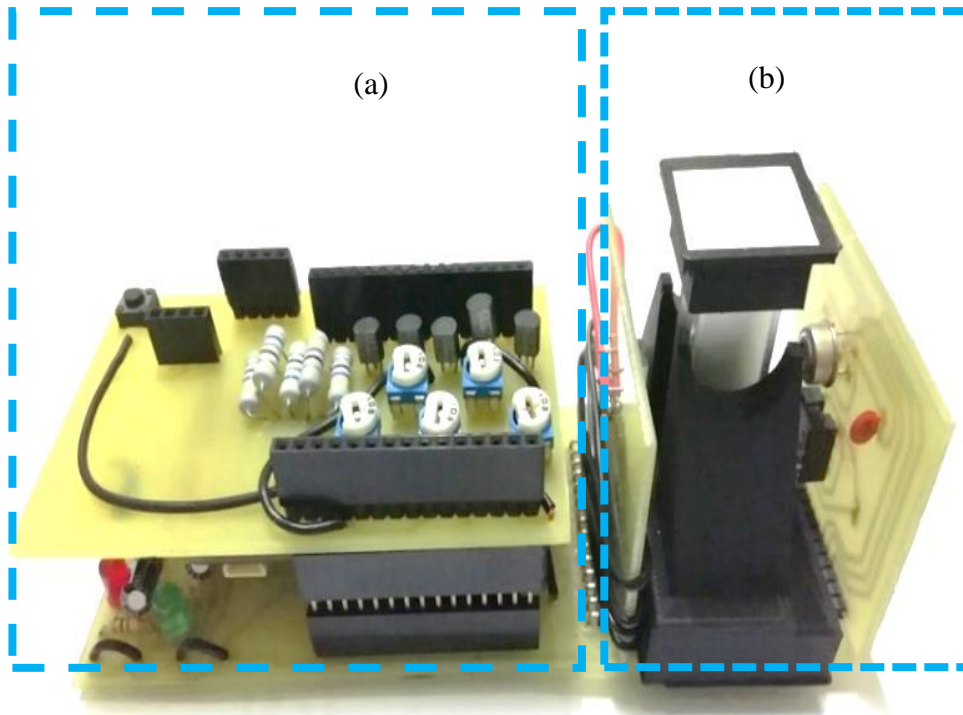


Fig. 1 - Prototype data acquisition measurement device (a) control circuit that consists of a microcontroller, five variable resistors, five transistors, one push button, and resistors; and (b) measurement part that consists of a photodiode, a multiple wavelength LED, a cuvette

2.3 pH and TAN measurement

Both the pH and TAN of a sample were measured immediately after the NIR spectral data acquisition of the sample was completed. First, the pH of the water sample in the cuvette was measured using a portable pH meter (HANNA® instruments). Next, Freshwater Master Test Kit (a salicylate-based ammonia test kit manufactured by Aquarium Pharmaceutical) was used as a convenient way to measure TAN. The water sample was mixed with the test kit solution according to the instructions provided, i.e. 5 ml of water sample was mixed with eight drops of each Ammonia test solution and then shaken for five seconds. After waiting for five minutes, the TAN value of the water sample can be estimated by comparing the final color of the water sample with the given ammonia color chart. This salicylate-based ammonia test kit measures the TAN value in parts per million (ppm), which is equivalent to milligrams per liter (mg/L), ranging from 0 to 8ppm.

2.4 Artificial Neural Network (ANN)

In this study, MATLAB software with Neural Network Toolbox was used to build the model ANN for predicting pH and TAN using the acquired NIR light and pH and TAN values. Holdout validation was used, i.e. the acquired data were randomly divided into training (50% or 132 data), validation (20% or 53 data), and testing (30% or 79 data) sets. The ANN that has a single hidden layer with a sigmoid activation function and a single output layer with a linear activation function was used in this study. The learning algorithm was Levenberg-Marquardt backpropagation. ANNs with different hidden neurons (i.e. one to five) were studied to optimize the complexity of the network by avoiding both overfitting and underfitting. The architecture of ANN is shown in Fig. 2. In this study, two ANN with the same architecture were trained to predict pH and TAN, respectively. ANN was re-trained with 100 different initial weights for different hidden neurons to identify the best prediction model for each neuron by avoiding local minima during the training process. This is because the initial weights and bias values of ANN are randomly assigned, which affect the performance of ANN. Therefore, by repeating the training process, the optimal values for initial weights and bias can be found. The performance metrics of pH and TAN prediction were evaluated using mean squared error (MSE) and correlation coefficient (R). Equations (1) and (2) are the general mathematical model for the pH and TAN prediction, respectively.

$$pH = b_1 I_{670} + b_2 I_{770} + b_3 I_{810} + b_4 I_{950} + c \quad (1)$$

$$TAN = g_1 /_{670} + g_2 /_{770} + g_3 /_{810} + g_4 /_{950} + d \tag{2}$$

Where, λ_{670} , λ_{770} , λ_{810} and λ_{950} are the four measured transmittance values that were used as the input of the ANN; β_1 , β_2 , β_3 , β_4 , and c are coefficient and constant values that estimated by ANN for pH prediction; while γ_1 , γ_2 , γ_3 , γ_4 , and d are coefficients and constant values estimated by ANN for TAN prediction.

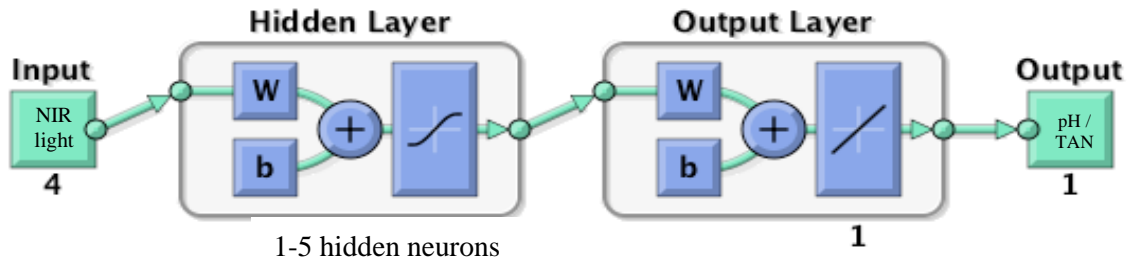


Fig. 2 – Artificial Neural Network (ANN) architecture

3. Results and Discussion

3.1 Spectral Data Samples Analysis

Fig. 3 shows the distribution of all pH and TAN values of 264 water samples. The measured pH and TAN of the water samples ranged from 5.01 to 7.11 and from 0 to 4 ppm, respectively. The TAN value was inversely proportional to the pH value, which ranged from five to seven. In other words, the higher the TAN value, the lower the pH of the water sample. This is in-line with the relationship between pH and the TAN value, in which water with a pH below 6.0 or exceed 8.5 has no beneficial bacteria to support the Nitrogen cycle, causing the TAN value to increase proportionally. This also suggests that pH measurement can be used for water quality screening purposes to save the time and cost of conventional TAN measurement.

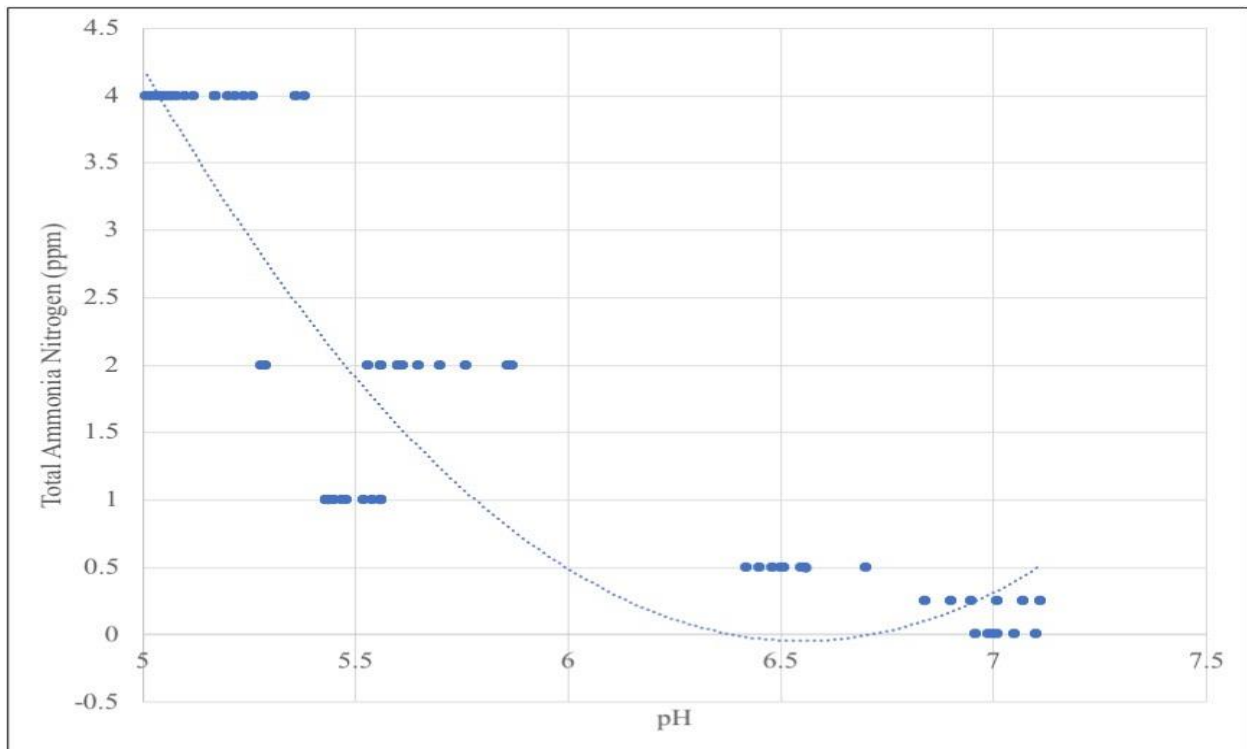


Fig. 3 - Total Ammonia Nitrogen against pH value for 264 data of water samples

Table 1 summarizes the descriptive statistics of the acquired transmitted light intensity with respect to the four different wavelengths. The signal at 770 nm appears to have the best correlation with pH and TAN, followed by 810, 950 and 670 nm, based on their standard deviation of transmitted light intensity. Nevertheless, since the NIR signals are highly correlated, a machine learning algorithm is needed to produce a multivariable predictive model.

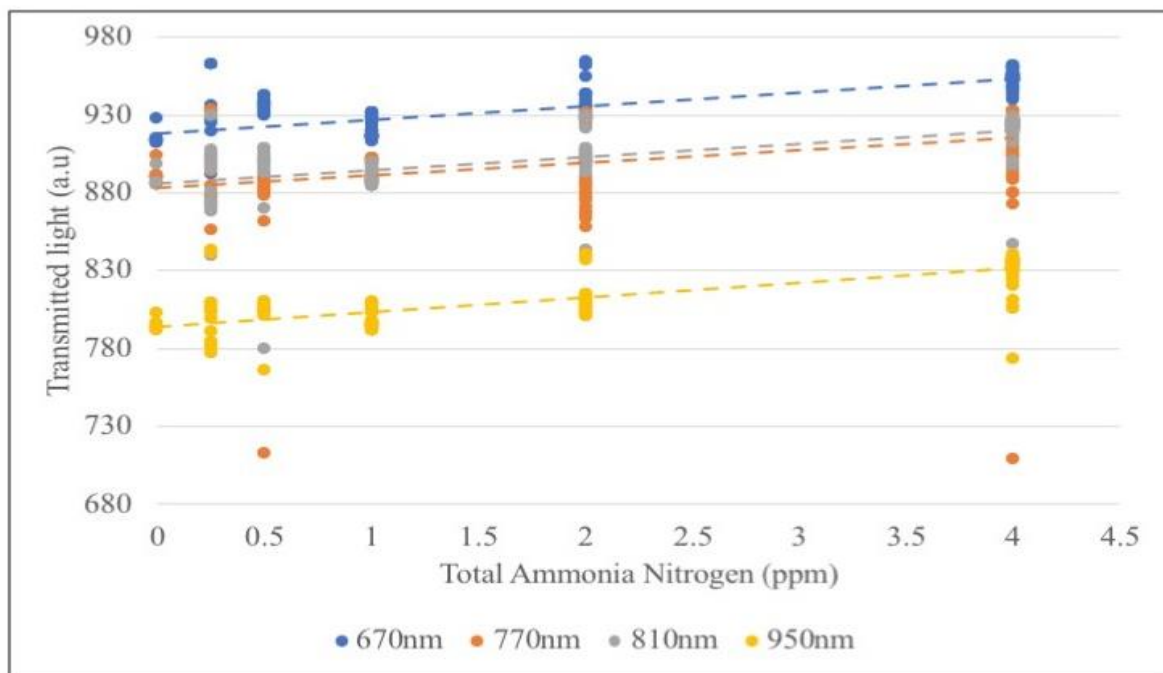
Table 1 - Descriptive statistics of the acquired transmitted light intensity for the 264 water samples

Wavelength (nm)	Minimum (a.u.)	Maximum (a.u.)	Mean (a.u.)	Standard deviation (a.u.)
670	892.4	964.6	936.9	16.9
770	709.2	933.6	900.6	25.4
810	780.0	929.8	904.5	18.7
950	765.6	842.8	814.0	18.0

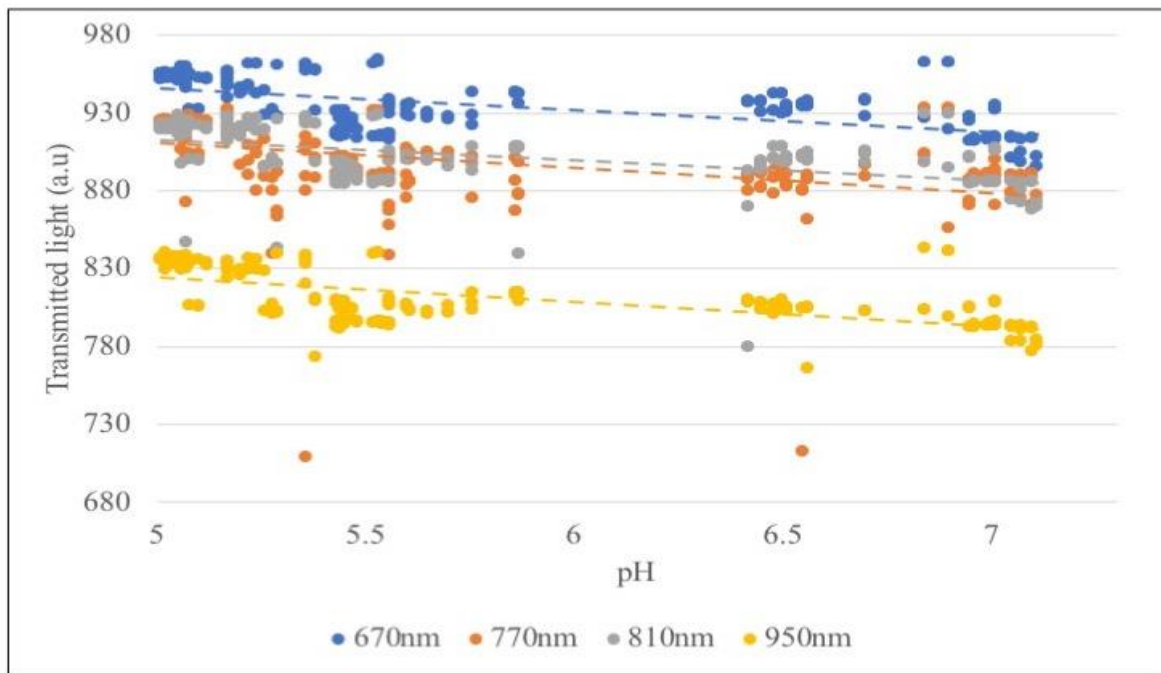
Fig. 4(a) shows the relationship between the four transmitted NIR intensities and the measured TAN values. The results show that the transmitted light intensity was directly proportional to the TAN value, i.e. the higher the TAN value of a water sample, the higher the transmitted light intensity (less NIR energy absorbed by the molecules in the water sample). When the TAN value was high (i.e. 2 to 4ppm), the pH value was in the lower range (i.e. below pH 6 as shown in Fig. 3), thus more unionized ammonia molecules were available to compare with ammonium ion. This could be due to fewer O-H bonding are available. Ammonium ion consists of one Nitrogen atom and four Hydrogen atoms, i.e. four N-H bonds, while unionized ammonia has three N-H bonds. In other words, ammonia, which has fewer N-H bonds, absorb less energy than ammonium ion. The reaction of ammonia in water is shown in Equation (3).



Next, Fig. 4(b) shows the four transmitted NIR intensities versus the measured pH of the water samples. The results show that the transmitted NIR intensity was inversely proportional to the measured pH, i.e. the transmitted light intensity decreased when the pH was increased. This could be due to the fact that the amount of -OH bond in water was lower, while the amount of H⁺ ion was higher when the pH was between 5.01 and 6.00 (i.e. in the acidic range). As mentioned above in Equation (3), in a low pH value, the presence of TAN was in ammonia molecule that absorbed less NIR energy compared with ammonium ion and hydroxyl ion. Thus, more energy was transmitted. Consequently, water samples that have a higher amount of hydroxyl ions (-OH) would absorb more NIR energy than water samples that have a less amount of -OH ion. In other words, more NIR energy was transmitted through the water samples with low pH values at a given wavelength.



(a)



(b)

Fig. 4 - The acquired NIR transmittance values against (a) Total Ammonia Nitrogen and (b) pH value

This is worth highlighting that the complexity of the water samples used in this study was high in nature as it was directly taken from the aquarium tank. Nevertheless, since NIR light is affected by C-H, O-H, and N-H bonds, other natural substances, e.g. CO₂, N₂, and O₂ may have insignificant effects on the acquired NIR signals that are transmitted through the water samples. Thus, this is aligned with the acquired NIR intensity that shows a linear relationship with TAN and pH values in Fig. 4.

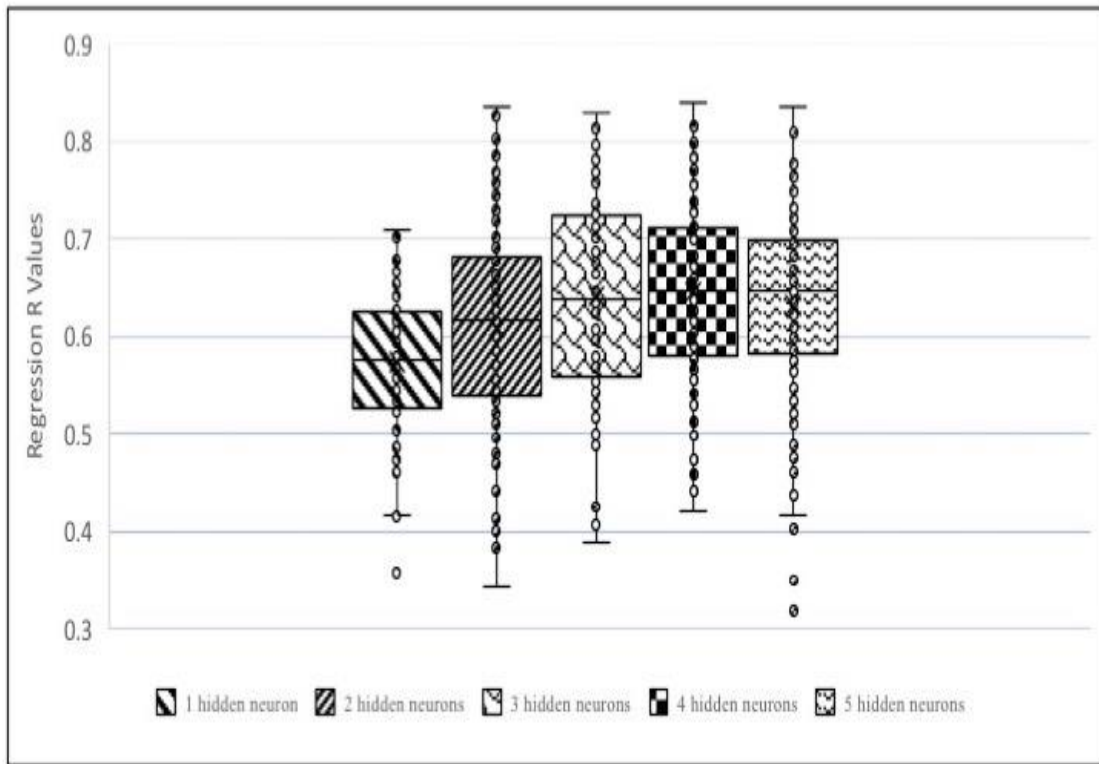
3.2 The Effects of Hidden Neuron Number

Fig. 5(a) shows the boxplot of the correlation coefficient for pH prediction when ANN used different hidden neurons and different initial weights. ANN with different initial weights achieved different performances because the ANN may be under-fitted if the best initial condition was not identified. The best testing regression values for ANN models that used two to five hidden neurons were higher than 0.8, i.e. 0.826, 0.814, 0.839, and 0.808, respectively. ANN that used four hidden neurons was the best model because the testing regression value was the highest. The selection of the number of hidden neurons was stopped at five. This is because the testing correlation performance showed no difference or decreased when more than four hidden neurons were used.

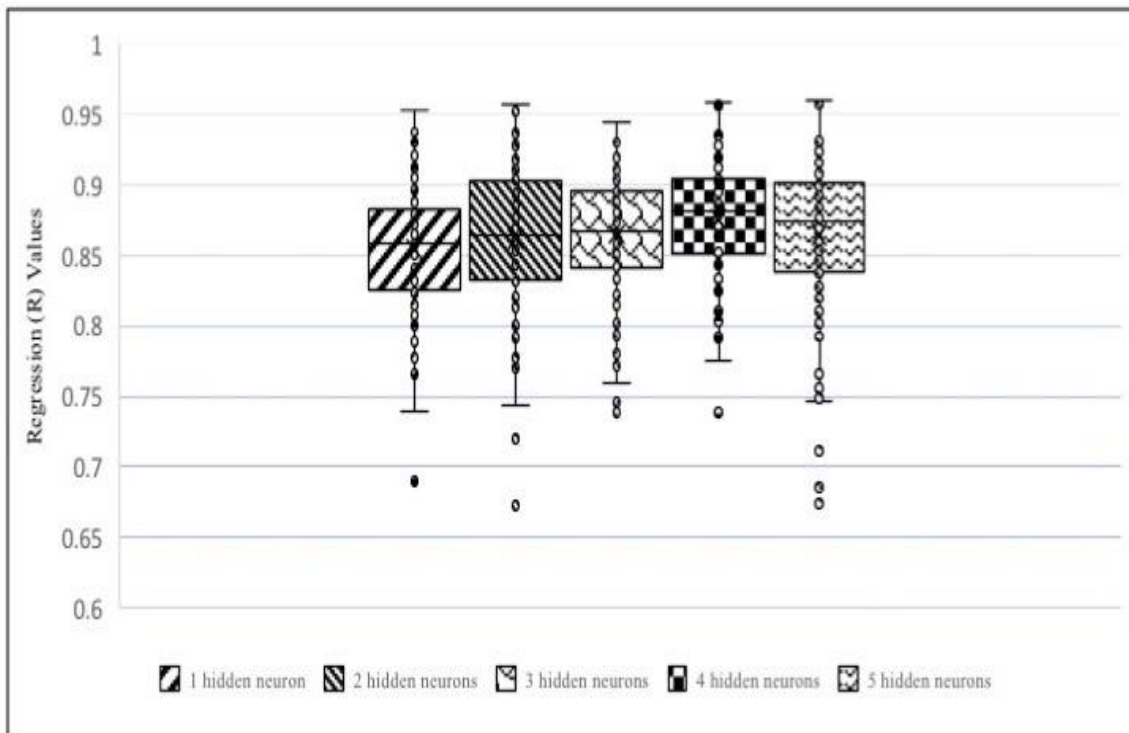
Fig. 5(b) shows the boxplot of the correlation coefficient for the TAN value prediction when ANN used different hidden neurons between one to five and different initial weights. A similar observation was made, i.e. ANN with different initial weights achieved different accuracy. This shows that it is necessary to create enough ANN with different initial conditions to avoid possible underfitting. The relationship established by ANN between TAN and transmission value was strong, i.e. the correlation coefficient was higher than 0.9. ANN, which used four hidden neurons, achieved the best prediction with the highest correlation coefficient of 0.839 for pH prediction and that of 0.956 for TAN prediction. The results show that TAN has a stronger correlation than the pH with the transmitted NIR energy. This could be due to the structure of TAN and pH, the former being proportional to the amount of N-H bonding, while the latter is proportional to the activation of hydrogen ion concentration.

Table 2 shows the mean square error (MSE) of ANN, which used different hidden neurons to predict the pH and concentration of TAN. Using the testing data for evaluation, the MSEs of ANNs that used one, two, three, four, and five hidden neurons for pH prediction were less than 0.28, i.e. 0.272, 0.160, 0.189, 0.146, and 0.177, respectively. ANN, which used four hidden neurons, achieved the lowest MSE in the training, validation, and testing evaluation, i.e. 0.097, 0.161, and 0.146 ppm², respectively. The testing MSE of ANN, which used different hidden neurons (i.e., from one to five) for TAN prediction, was less than 0.51 ppm². ANN that used four hidden neurons achieved the lowest MSE in the

training, validation, and testing evaluation, i.e. 0.271, 0.389, and 0.313 ppm², respectively. Thus, ANN with four hidden neurons achieved the best performance in predicting both water pH and TAN.



(a)



(b)

Fig. 5 - Boxplot for the testing results - the correlation coefficient (R-value) versus the number of hidden neurons: (a) pH and (b) Total Ammonia Nitrogen prediction

Table 2 - The performance of ANN with respect to different hidden neurons for pH and Total Ammonia Nitrogen prediction

Number of Hidden Neuron	Mean Square Error					
	pH			Total Ammonia Nitrogen (ppm ²)		
	Training	Validation	Testing	Training	Validation	Testing
1	0.293	0.283	0.272	0.759	0.477	0.421
2	0.237	0.183	0.160	0.358	0.773	0.438
3	0.135	0.273	0.190	0.308	0.232	0.509
4	0.097	0.162	0.147	0.271	0.390	0.314
5	0.137	0.163	0.178	0.210	0.256	0.496

4. Conclusion

A new approach that adapted NIR spectroscopic concept to predict water pH and TAN was developed and evaluated. The developed prototype can measure four NIR transmittance values of different wavelengths (i.e., 670, 770, 810, and 950 nm) with one photodiode. An inverse relationship between pH and TAN was observed when the pH values were between five and seven. ANN was used to establish the relationship between the acquired transmitted NIR light and pH and TAN of water. This proposed system was able to predict the pH of water with a correlation coefficient and MSE of 0.839 and 0.146. A better performance was achieved in predicting the TAN of water with a correlation coefficient value and MSE of 0.956 and 0.313 ppm², respectively. This shows that ANN coupled with NIR light is promising for in situ prediction of pH and TAN of water. In the future, the proposed system can be adapted for the prediction of other interesting water constituents and components of interest, and the performance can be further improved using different hyperparameter optimization strategies.

For future work, researchers will investigate different parameter optimization algorithms from ANN to automate the hyperparameter optimization process. Additionally, it is recommended that future study may evaluate the use of transfer learning (TL) algorithms in related research. TL is a different approach compared to classical machine learning. The TL algorithm transfers the learning knowledge of different domain features or attributes of the source dataset to the target dataset. Consequently, by using the TL algorithm, a smaller dataset is expected to be sufficient to achieve good performance, which is usually achieved with more data when classical machine learning is used. Moreover, with a suitable TL algorithm, the accuracy of the prediction model could be further improved.

Acknowledgement

This research was supported by Ministry of Higher Education (MOHE) through Fundamental Research Grant Scheme (FRGS) FRGS/1/2020/ICT02/UTHM/03/6. Authors would like to acknowledge Faculty of Electrical and Electronic Engineering (FKEE), Universiti Tun Hussein Onn Malaysia (UTHM), and Universiti Tun Hussein Onn Malaysia (UTHM) for providing facilities and resources to this study.

References

- [1] S. Jennings *et al.*, "Aquatic food security: insights into challenges and solutions from an analysis of interactions between fisheries, aquaculture, food safety, human health, fish and human welfare, economy and environment," *Fish Fish.*, vol. 17, no. 4, pp. 893–938, Dec. 2016, doi: 10.1111/faf.12152.
- [2] J. Beddington, "Food security: Contributions from science to a new and greener revolution," *Philosophical Transactions of the Royal Society B: Biological Sciences*, vol. 365, no. 1537. Royal Society, pp. 61–71, Jan. 2010, doi: 10.1098/rstb.2009.0201.
- [3] R. L. Naylor *et al.*, "Effect of aquaculture on world fish supplies," *Nature*, vol. 405, no. 6790, pp. 1017–1024, Jun. 2000, doi: 10.1038/35016500.
- [4] T. J. Park *et al.*, "Development of water quality criteria of ammonia for protecting aquatic life in freshwater using species sensitivity distribution method," *Sci. Total Environ.*, vol. 634, pp. 934–940, Sep. 2018, doi: 10.1016/j.scitotenv.2018.04.018.
- [5] H. L. Galasso, M. D. Callier, D. Bastianelli, J.-P. Blancheton, and C. Aliaume, "The potential of near infrared spectroscopy (NIRS) to measure the chemical composition of aquaculture solid waste," *Aquaculture*, vol. 476, pp. 134–140, Jul. 2017, doi: 10.1016/J.AQUACULTURE.2017.02.035.

- [6] J. T. Alander, V. Bochko, B. Martinkauppi, S. Saranwong, and T. Mantere, "A Review of Optical Nondestructive Visual and Near-Infrared Methods for Food Quality and Safety," vol. 2013, 2013.
- [7] F. Yuan, Y. Huang, X. Chen, and E. Cheng, "A Biological Sensor System Using Computer Vision for Water Quality Monitoring," *IEEE Access*, vol. 6, pp. 61535–61546, 2018, doi: 10.1109/ACCESS.2018.2876336.
- [8] Yokogawa, "pH in fish farming," *Yokogawa Electric Corporation*, pp. 9–11, 2014.
- [9] S. Karastogianni, S. Girousi, and S. Sotiropoulos, *pH: Principles and Measurement*, 1st ed. Elsevier Ltd., 2016.
- [10] M. Li, S. Gong, Q. Li, L. Yuan, F. Meng, and R. Wang, "Ammonia toxicity induces glutamine accumulation, oxidative stress and immunosuppression in juvenile yellow catfish *Pelteobagrus fulvidraco*," *Comp. Biochem. Physiol. Part - C Toxicol. Pharmacol.*, vol. 183–184, pp. 1–6, 2016, doi: 10.1016/j.cbpc.2016.01.005.
- [11] C. E. Boyd, C. S. Tucker, and R. Viriyatum, "Interpretation of pH, Acidity, and Alkalinity in Aquaculture and Fisheries," *N. Am. J. Aquac.*, vol. 73, no. 4, pp. 403–408, Oct. 2011, doi: 10.1080/15222055.2011.620861.
- [12] "Aquarium Water pH Maintenance."
- [13] A. H. Ringwood and C. J. Keppler, "Water quality variation and clam growth: Is pH really a non-issue in estuaries?," *Estuaries*, vol. 25, no. 5, pp. 901–907, 2002, doi: 10.1007/BF02691338.
- [14] A. A. Yusof, S. Bakri, and S. Misha, "TDS and pH analysis for water quality monitoring in water hydraulics food processor," *Int. J. Integr. Eng.*, vol. 11, no. 4, pp. 218–224, 2019, doi: 10.30880/ijie.2019.11.04.024.
- [15] L. Zhou and C. E. Boyd, "An assessment of total ammonia nitrogen concentration in Alabama (USA) ictalurid catfish ponds and the possible risk of ammonia toxicity," *Aquaculture*, vol. 437, pp. 263–269, Feb. 2015, doi: 10.1016/j.aquaculture.2014.12.001.
- [16] J. Ogbonna and Chinonso A, "Determination of the concentration of ammonia that could have lethal effect on fish pond," *ARNP J. Eng. Appl. Sci.*, vol. 5, no. 2, pp. 1–6, 2006.
- [17] N. Goldshleger, A. Grinberg, S. Harpaz, A. Shulzinger, and A. Abramovich, "Real-time advanced spectroscopic monitoring of Ammonia concentration in water," *Aquac. Eng.*, vol. 83, pp. 103–108, 2018, doi: 10.1016/j.aquaeng.2018.10.002.
- [18] D. P. Sartory and J. Watkins, "Conventional culture for water quality assessment: is there a future?," *J. Appl. Microbiol.*, vol. 85, no. S1, pp. 225S–233S, Dec. 1998, doi: 10.1111/j.1365-2672.1998.tb05302.x.
- [19] A. Demeke and A. Tassew, "A review on water quality and its impact on Fish health," *Int. J. Fauna Biol. Stud.*, vol. 3, no. 1, pp. 21–31, 2016.
- [20] A. Morellos *et al.*, "Machine learning based prediction of soil total nitrogen, organic carbon and moisture content by using VIS-NIR spectroscopy," *Biosyst. Eng.*, vol. 152, pp. 104–116, 2016, doi: 10.1016/j.biosystemseng.2016.04.018.
- [21] J. Zhou, X. Wu, Z. Chen, J. You, and S. Xiong, "Evaluation of freshness in freshwater fish based on near infrared reflectance spectroscopy and chemometrics," *LWT*, vol. 106, pp. 145–150, Jun. 2019, doi: 10.1016/J.LWT.2019.01.056.
- [22] A. O' Reilly, R. Coffey, A. Gowen, and E. Cummins, "Evaluation of near-infrared chemical imaging for the prediction of surface water quality parameters," *Int. J. Environ. Anal. Chem.*, vol. 95, no. 5, pp. 403–418, Apr. 2015, doi: 10.1080/03067319.2015.1025222.
- [23] P. B. Skou, T. A. Berg, S. D. Aunbjerg, D. Thaysen, M. A. Rasmussen, and F. van den Berg, "Monitoring process water quality using near infrared spectroscopy and partial least squares regression with prediction uncertainty estimation," *Appl. Spectrosc.*, vol. 71, no. 3, pp. 410–421, 2017, doi: 10.1177/0003702816654165.
- [24] S. S. Chong, A. R. Abdul Aziz, and S. W. Harun, "Fibre optic sensors for selected wastewater characteristics," *Sensors (Switzerland)*, vol. 13, no. 7, pp. 8640–8668, 2013, doi: 10.3390/s130708640.
- [25] W. Tang, W. Yan, G. He, G. Li, and L. Lin, "Dynamic spectrum nonlinear modeling of VIS & NIR band based on RBF neural network for noninvasive blood component analysis to consider the effects of scattering," *Infrared Phys. Technol.*, vol. 96, no. November 2018, pp. 77–83, 2019, doi: 10.1016/j.infrared.2018.11.018.
- [26] C. Cui and T. Fearn, "Modern practical convolutional neural networks for multivariate regression: Applications to NIR calibration," *Chemom. Intell. Lab. Syst.*, vol. 182, pp. 9–20, 2018, doi: 10.1016/j.chemolab.2018.07.008.
- [27] K. Ncama, S. Z. Tesfay, O. A. Fawole, U. L. Opara, and L. S. Magwaza, "Non-destructive prediction of 'Marsh' grapefruit susceptibility to postharvest rind pitting disorder using reflectance Vis/NIR spectroscopy," *Sci. Hortic. (Amsterdam)*, vol. 231, no. August 2017, pp. 265–271, 2018, doi: 10.1016/j.scienta.2017.12.028.
- [28] E. S. Mohamed, A. M. Saleh, A. B. Belal, and A. A. Gad, "Application of near-infrared reflectance for quantitative assessment of soil properties," *Egypt. J. Remote Sens. Sp. Sci.*, vol. 21, no. 1, pp. 1–14, 2018, doi: 10.1016/j.ejrs.2017.02.001.
- [29] E. Tamburini, F. Vincenzi, S. Costa, P. Mantovi, P. Pedrini, and G. Castaldelli, "Effects of moisture and particle size on quantitative determination of total organic carbon (TOC) in soils using near-infrared spectroscopy," *Sensors (Switzerland)*, vol. 17, no. 10, pp. 1–15, 2017, doi: 10.3390/s17102366.
- [30] N. A. S. Suarin, K. S. Chia, and S. F. Z. Mohamad Fuzi, "A Portable in-situ near-infrared LEDs-based soil Nitrogen sensor using artificial Neural Network," *Int. J. Integr. Eng.*, vol. 10, no. 4, pp. 81–87, 2018, doi: 10.30880/ijie.2018.10.04.013.
- [31] A. Azmi *et al.*, "Artificial neural network and wavelet features extraction applications in nitrate and sulphate

- water contamination estimation,” *Int. J. Integr. Eng.*, vol. 9, no. 4, pp. 64–75, 2017.
- [32] H. Mohammadi Lalabadi, M. Sadeghi, and S. A. Mireei, “Fish freshness categorization from eyes and gills color features using multi-class artificial neural network and support vector machines,” *Aquac. Eng.*, vol. 90, no. October 2019, p. 102076, 2020, doi: 10.1016/j.aquaeng.2020.102076.
- [33] P. Wang, X. Yan, and F. Zhao, “Multi-objective optimization of control parameters for a pressurized water reactor pressurizer using a genetic algorithm,” *Ann. Nucl. Energy*, vol. 124, pp. 9–20, 2019, doi: 10.1016/j.anucene.2018.09.026.
- [34] Y. Chen, X. Fang, L. Yang, Y. Liu, C. Gong, and Y. Di, “Artificial Neural Networks in the Prediction and Assessment for Water Quality: A Review,” in *Journal of Physics: Conference Series*, Jul. 2019, vol. 1237, no. 4, doi: 10.1088/1742-6596/1237/4/042051.
- [35] N. A. S. Suarin, K. S. Chia, and F. N. Kosmani, “Stingless Bee Honey Classification Using near Infrared Light Coupled with Artificial Neural Network,” in *2020 Zooming Innovation in Consumer Technologies Conference, ZINC 2020*, 2020, pp. 99–102, doi: 10.1109/ZINC50678.2020.9161785.